Available online at www.sciencedirect.com
ScienceDirect
Applied Surface Science xxx (2007) xxx–xxx
applied surface science
www.elsevier.com/locate/apsusc

# Electrostatic forces in micromanipulations: Review of analytical models and simulations including roughness

M. Sausse Lhernould [a,*], A. Delchambre [a], S. Régnier [b], P. Lambert [a]

[a] Université Libre de Bruxelles, BEAMS Department, CP165-14, Av. F.D. Roosevelt 50, B-1050 Bruxelles, Belgium
[b] Université Pierre et Marie Curie, Laboratoire de Robotique de Paris, Route du Panorama, BP 61, 92265 Fontenay Aux Roses, France

Received 29 September 2006; received in revised form 18 January 2007; accepted 18 January 2007

**Abstract**

Manipulations by contact of objects between 1 μm and 1 mm are often disturbed by adhesion between the manipulated object and the gripper. Electrostatic forces are among the phenomena responsible for this adhesive effect. Analytical models have been developed in the literature to predict the electrostatic forces. Most models are developed within the framework of scanning probe microscopy, i.e. for a contact between a conducting tip and a metallic surface. Models are reviewed in this work and compared with our own simulations using finite elements modeling. The results show a good correlation. The main advantage of our simulations lies in the fact that they can integrate roughness parameters. For this purpose, a fractal representation of the surface topography was chosen through the use of the Weierstrass-Mandelbrot function. Comparisons with experimental benchmarks from the literature show very good correlation between experimental results and simulations. It demonstrates the importance of surface topography on electrostatic forces at very close separation distances.


*PACS :* 41.20.Cv; 68.35.Np; 68.35.Ct

*Keywords:* Micromanipulations; Adhesion; Electrostatic forces; Roughness; Fractals

## 1. Introduction

This work was achieved within the framework of micromanipulations (i.e. manipulations of objects between 1 μm and 1 mm) with contact [1]. In this context, perturbations related to adhesive surface forces were observed. This leads sometimes to the impossibility of releasing the object. Beside contact and pull off forces, three main surface forces have been identified: capillary, van der Waals and electrostatic forces. Many attempts have already been made to evaluate them [2–5]. Electrostatic forces have been more specifically related to the jumping on contact phenomenon. It causes the object to jump on the gripper when trying to grasp it and may be responsible for an inaccurate positioning of the object between the end-effectors of the gripper. In the present work, the attention is focused on the electrostatic forces in the case of a contact between conducting materials. This restriction is due to the fact that to this date no reliable theory has been formulated on what happens during insulator–conductor and insulator–insulator contacts. When two metals are brought in proximity they acquire opposite charges through a process called contact charging. They exchange electrons in order for their Fermi levels to get to an equilibrium state. Electrostatic forces are therefore long range forces.

During micromanipulations, contact can be seen as occurring at the scale of the object (microscale) or at the scale of the surface roughness (nanoscale). The present work is mostly at the nanoscale because no experimental results are available at the microscale for electrostatic force measures. The applicative scale is, however, the microscale. The application is to find solutions for the design of a microgripper such as the one developed by ref. [6](Fig. 1) in order to avoid adhesion.

We investigate analytical models and develop our own simulation tool using the finite element software Comsol. The main advantage of the simulations is that it can integrate the surface topography factor through a fractal representation of

* Corresponding author. Tel.: +32 2 650 28 59; fax: +32 2 650 47 24.
*E-mail address:* msausse@ulb.ac.be (M. S. Lhernould).
*URL:* http://beams.ulb.ac.be

0169-4332/$ – see front matter © 2007 Elsevier B.V. All rights reserved.
doi:10.1016/j.apsusc.2007.01.098

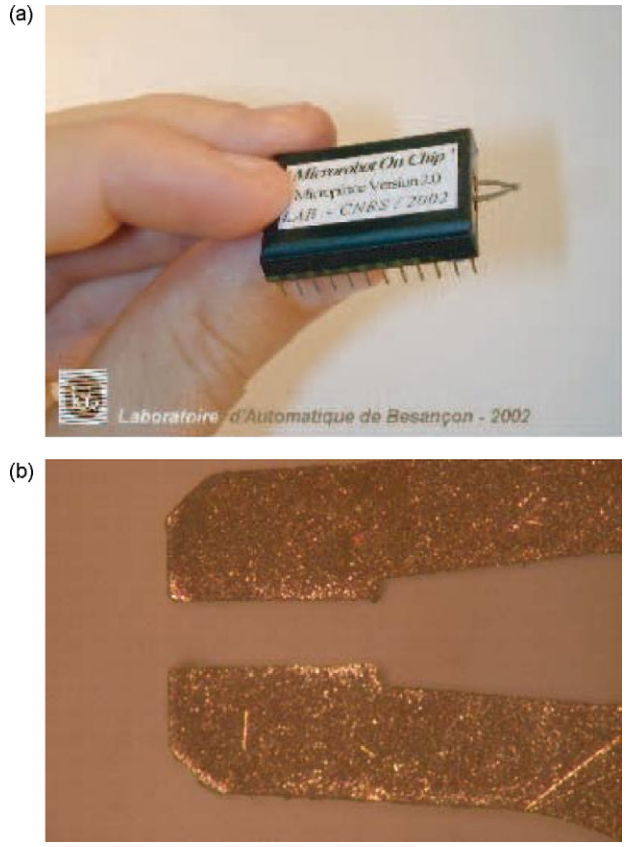


Fig. 1. Microgripper developed by the Laboratoire d'Automatique de Besançon (LAB) [6]: (a) gripper and (b) zoom on gripper.

the surface. The following section is a review of the available analytical models found in the literature for predicting the electrostatic forces. Most of these models have been developed within the framework of scanning probe microscopy for a conducting tip in proximity with a metallic surface. Most models are restricted in their applicable separation distance range. To go beyond the latter, we propose to make use of two-dimensional axisymetric finite elements simulations. The third section is dedicated to the modeling principles used for the simulations. The results obtained are compared with the analytical models. The main originality of the developed simulation tool is that it can integrate roughness parameters in order to include roughness factors in the simulations. We chose a fractal representation of the topography which is explained in the fourth section. It is indeed necessary to characterize rough surfaces by intrinsic parameters which are independent of all scales of roughness such as the fractal parameters. The results including roughness parameters are compared with experimental benchmarks of the literature in Section 5. An application case is given in Section 6.

## 2. Review of analytical models

The main assumption for the analytical models developed in literature is that the surfaces are smooth involving for the models not to take surface topography into account. This is a very strong assumption since, not matter how carefully or expensively a surface is manufactured, it can never be perfectly smooth. The second assumption defines the materials as conductive involving that the potential is uniformly distributed along the surface, the electric field is normal to the surface and the charges only carried by the surfaces of the materials (no volumic charges). The fact that no charge is present between the contacting objects is the third assumption. In Fig. 2, the different geometries involved in this work are presented, plane-plane contact, sphere-plane contact, sphere ended cone-plane contact and hyperbole-plane contact. The plane-plane model [7] gives the electrostatic pressure. The experience shows, however, that it is very difficult to determine the area of contact in real configurations. The planar model is thus very restricted in terms of applications. Three sphere models [7–12] have been developed from the general expression given by ref. [13], depending on the separation distance range. These models are often used to get a quantitative assessment of the electrostatic forces between the probe and the substrate in scanning probe microscopy. For conical tips, the uniformly charged line model [14] (where the cone is approximated by a charged line of constant charge density) and the asymptotic model [11] have been developed. An expression for the hyperboloid configuration has been given by refs. [15,16]. Finally, tilted conical tip models have also been presented by ref. [17] where the issue of the tilting angle in electrostatic interactions in AFM is discussed. The contribution of the cantilever has been considered by refs. [18,19]. Table 1 summarizes and briefly defines the different terms used. The analytic expressions are given in Table 2.

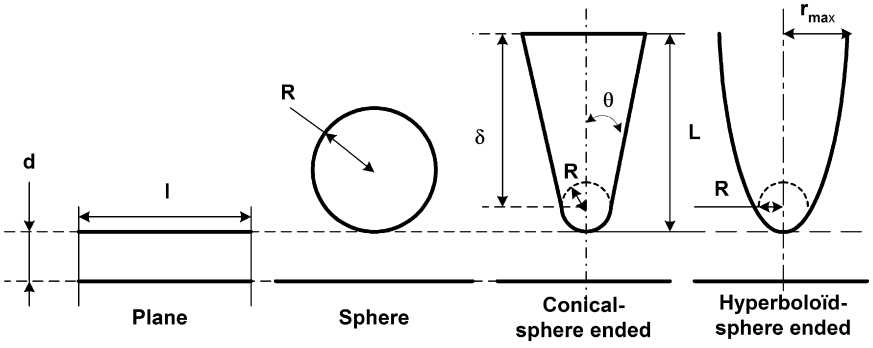


Fig. 2. Representation of the involved geometries.

Please cite this article in press as: M.S. Lhernould et al., Electrostatic forces in micromanipulations: Review of analytical models and simulations including roughness, Appl. Surf. Sci. (2007), doi:10.1016/j.apsusc.2007.01.098

Table 1
Definitions

| Term | Definition | Values |
|---|---|---|
| $\epsilon_0$ | Free space permittivity ($m^{-3}$ $kg^{-1}$ $s^4$ $A^2$) | $8.85 \times 10^{-12}$ |
| $\epsilon_r$ | Relative permittivity | 1.00054 for air |
| $R$ | Sphere radius (m) | 10 nm–100 μm |
| $d$ | Separation distance (m) | 1 nm–100 μm |
| $U$ | Potential difference (V) | 0.5–20 V |
| $\theta$ | Cone half aperture angle (rad) | Till 20° |
| $L$ | Length of tip (m) | 10–500 μm |
| $A$ | Area of contact ($m^2$) | |
| $r_{max}$ | Maximum distance to the axis (m) | |
| $\delta$ | Truncated cone height (m) | |
| $l$ | Plane width (m) | |

## 3. Simulation tool

During micromanipulations the contact potential difference (CPD) between the gripper and the manipulated object depends on the intrinsic properties of the materials in the case of conducting materials. Electrons in a metal have a certain energy level and stay in the metal at rest. There is a minimum energy level defined for each metal that its electrons have to acquire in order to be able to leave it. This energy is defined as the work function. Two pieces of different metals placed sufficiently close to exchange electrons will reach thermodynamic equilibrium by equalizing the height of their Fermi levels. Equilibrium is reached by the establishment of a contact potential. The result is an attractive electrostatic force between the objects in proximity. The electric potential $U$ in the surrounding environment obeys Laplace's equation:

$$\Delta U = 0 \tag{1}$$

The electric field is obtained from the gradient of $U$.

$$E = -\text{grad}\, U \tag{2}$$

A two-dimensional axisymetric simulation is performed using the commercial simulation tool Comsol to model the geometry and to solve the partial differential equation Eq. (1) with the finite elements method. The outer boundary conditions insure the electric insulation of the domain which results in no normal component of the electric field on the outer boundaries. The potential $U$ is applied on the boundary delimiting the tip in order to simulate the potential difference between the tip and the surface while the contacting flat surface is grounded (see Fig. 3). The electrostatic pressure is calculated using Eq. (3).

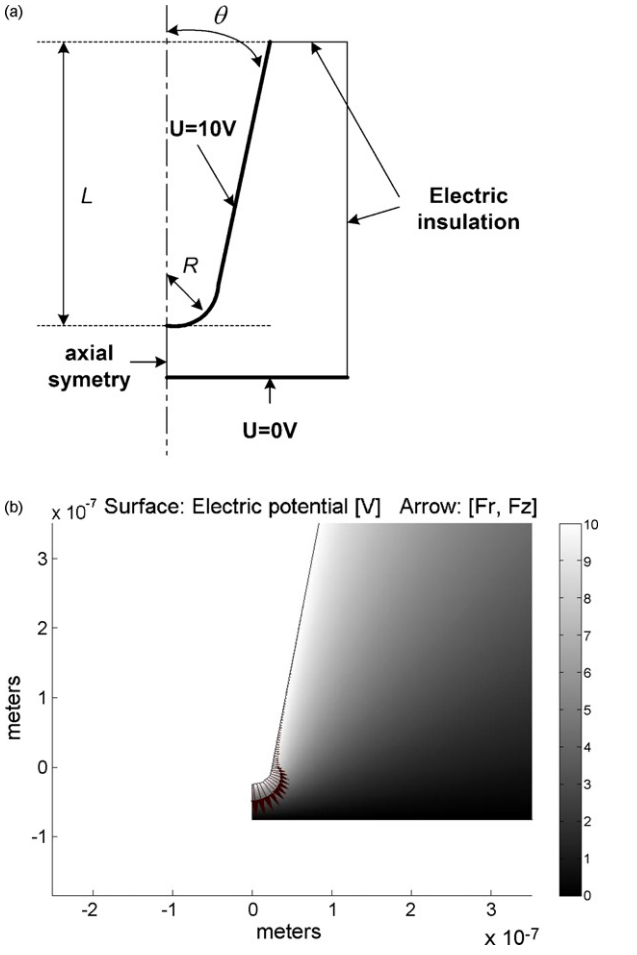


Fig. 3. Simulation of a contact between a conical tip and a plane: (a) modelling and (b) solution.

$$F_{elec} = \frac{\epsilon_0 \epsilon_r E^2}{2} \tag{3}$$

Table 2
Review of analytical models

| Contact type | Expression | Refs. |
|---|---|---|
| Plane-plane | $F_{plane} = \frac{\epsilon_0 U^2 A}{2d^2}$ | [7] |
| Sphere-plane | $F_{sphere1} = \frac{\pi\epsilon_0 R U^2}{d}$ for $R \gg d$ | [7–10] |
| Sphere-plane | $F_{sphere2} = \frac{\pi\epsilon_0 R^2 U^2}{d^2}$ for $R \gg d$ | [10,11] |
| Sphere-plane | $F_{sphere3} = \pi\epsilon_0 \frac{R^2 U^2}{d(d+R)}$ for $R \ll d \ll L$ | [11,12] |
| Conical tip (charged line) | $F_{ch} \cong \frac{\lambda_0^2}{4\pi\epsilon_0} \ln\left(\frac{L}{4d}\right)$ for $R \gg d$ with $\lambda_0 = 4\pi\epsilon_0 U \left[\ln\left(\frac{1+\cos\theta}{1-\cos\theta}\right)\right]^{-1}$ | [14] |
| Conical tip (asymptotic) | $F_{as} = \pi\epsilon_0 U^2 \left[\frac{R^2(1-\sin\theta)}{d[d+R(1-\sin\theta)]} + k^2\left(\ln\frac{L}{d+R(1-\sin\theta)} - 1 + \frac{R\cos^2\theta\sin\theta}{d+R(1-\sin\theta)}\right)\right]$ with $k^2 = \frac{1}{[\ln(\tan(\theta/2))]^2}$ | [11] |
| Hyperboloid tip | $F_{hyp1} = \pi\epsilon_0 U^2 k^2 \left[\ln\left(1+\frac{L}{R}\right) - \frac{(d-R/\tan\theta^2)L}{d(L+d)}\right]$ with $k^2 = \frac{1}{[\ln(\tan(\theta/2))]^2}$ | [19] |
| Hyperboloid tip | $F_{hyp2} = 4\pi\epsilon_0 U^2 \frac{\ln\left[1+(r_{max}/R)^2(1+(R/d))\right]}{\ln^2((1+\eta_{tip})/(1-\eta_{tip}))}$ with $\eta_{tip} = \sqrt{\frac{d}{d+R}}$ | [15,16] |

Please cite this article in press as: M.S. Lhernould et al., Electrostatic forces in micromanipulations: Review of analytical models and simulations including roughness, Appl. Surf. Sci. (2007), doi:10.1016/j.apsusc.2007.01.098

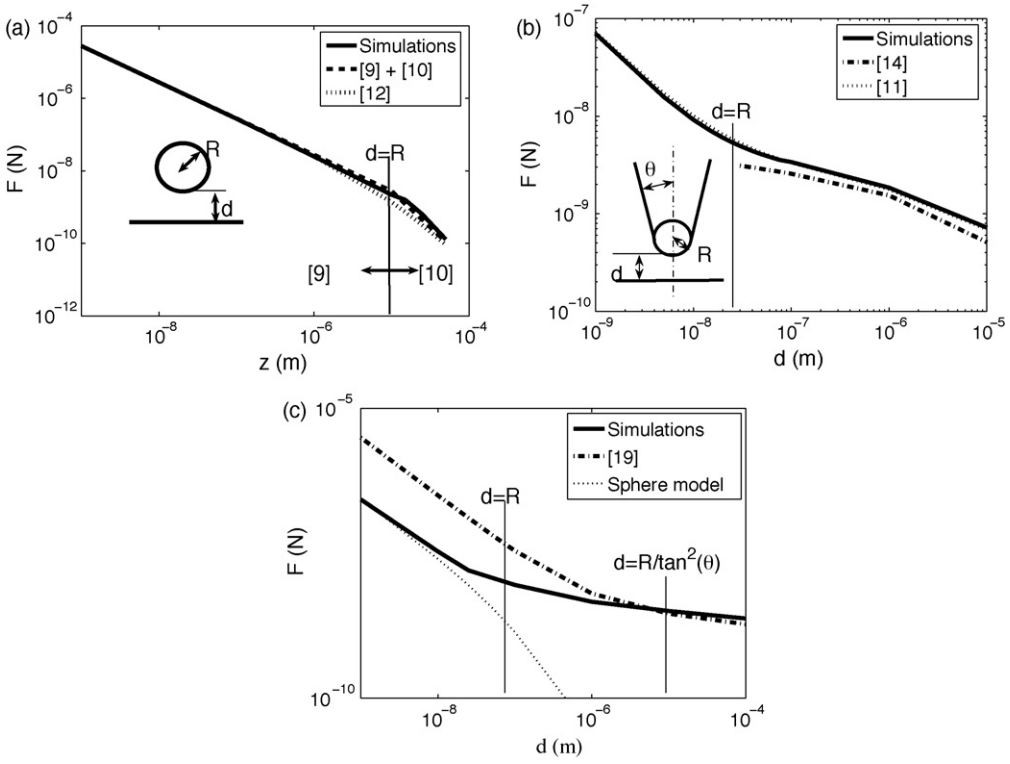


Fig. 4. (a) Validation of simulations with the sphere models for a sphere of radius 10 μm and a potential difference $U = 10$ V. (b) Validation of simulations with the conical models for dimensions of the tip $L = 125$ μm, $R = 25$ nm, $\theta = 9.46°$ (half aperture angle) and a potential difference $U = 10$ V. (c) Validation of simulations with the hyperboloid model for $R = 100$ nm, $\theta = 6°$ and a potential difference $U = 10$ V.

We are able to calculate the total force acting on the two geometries by integrating the force for all the contributions brought by each element in the model.

### 3.1. Validation

In order to compare simulations results and analytical models, the electrostatic force is plotted as a function of the separation distance. This is done for a wide range of separation distances in order to visualize eventual restrictions. As we observed in the reviewing part of this work, the main restriction for most analytical models lies in the range of applicable separation distances. For the plane-plane contact, the results between simulations and analytic formulation are in perfect correlation with less than 1% error. For the sphere-plane contact, Fig. 4 a also shows a very good correlation between analytic expressions and simulations even though errors start to appear for large separation distances ($d = R$). Please refer to Table 2 for the analytic expressions of the different models. For the sphere ended-conical geometry, the results depend on the used model. From Fig. 4 b, and as expected by the restrictions of the model, the uniformly charged line model only correlates simulations for separation distances larger than the apex radius (reliability interval of the model). We observe a very good correlation between the asymptotic model and the simulations on all separation distances range. Further simulations showed that modifying the length, aperture angle or tip radius does not significantly influence the accuracy of the results. The hyperboloid model overestimates the force compared to simulations especially at small separation distances (Fig. 4c). This correlates the reliability interval provided by ref. [19]. The model is exact for $d = R/(\tan\theta)^2$, i.e. at long separation distances in our application case. At very small separation distances, even if the tip is modeled as an hyperboloid, only the spherical extremity contributes to the electrostatic forces and results should agree with the sphere model.

### 3.2. Conclusion

Due to the good correspondence between models and simulations, it can be concluded that a reliable electrostatic forces simulation tool has been developed. It will allow us to investigate more complex geometries. The difficulty in developing an analytical model is to accurately define the charge repartition on the bodies in contact and particularly on the conical part of a sphere-ended conical tip. All conical models (except for the uniformly charged line model) are accurate for small separation distances. Developing the simulation tool not only gives an estimation on the intensity of the forces but also the charge repartition on the solids and thus the force repartition. The analytical models reviewed have mostly been developed within the scope of evaluating electrostatic forces in scanning force microscopy experiments. All of them have been validated experimentally by their authors. The errors observed between experimental measures and results from the analytic expressions is partly attributed to the approximation made in the representation of the geometry.

Please cite this article in press as: M.S. Lhernould et al., Electrostatic forces in micromanipulations: Review of analytical models and simulations including roughness, Appl. Surf. Sci. (2007), doi:10.1016/j.apsusc.2007.01.098

Geometries integrated in the calculation do not indeed always perfectly reflect the real shape of the tip.

The advantages of developing a simulation tool are, in the context of micromanipulator design, to be able to take into account more parameters and more complex ones. These include not only the geometry of the end-effectors, the geometry of the handled object and the materials, but also the fabrication process and surface treatments (polishing, roughening, coating) thanks to the introduction of surface topography parameters. The simulations have also the advantage that they will allow us to introduce deformed geometries in future studies. This is illustrated in Fig. 9.

Another explanation for the discrepancy between experimental results and analytical results may be attributed to surface roughness which may also have an influence on the measures. This is investigated in the next sections of this work.

## 4. Roughness representation: The Weierstrass Mandelbrot function

In order to integrate the roughness factor in simulations, a fractal representation is used. Fractals are irregular objects possessing similar geometrical characteristics at all scales. This characteristic is called self-similarity. The geometries of fractal surfaces are also continuous and non-differentiable. The profile of rough surfaces is being assumed to be continuous even at the smallest scales. Ever-finer levels of detail appears under repeated magnificence. The tangent at any point cannot be defined and the profile has the mathematical property of being continuous everywhere but non-differentiable at all points. The Weirstrass-Mandelbrot function satisfies the properties of continuity, non-differentiability and self-similarity [20] and is therefore used to simulate such profiles.

$$z(x) = L\left(\frac{G}{L}\right)^{D-1} \sum_{n=0}^{\infty} \frac{\cos\left(2\pi\gamma^n \frac{x}{L}\right)}{\gamma^{(2-D)n}} \tag{4}$$

where $L$ is the fractal sample length, $D$ the fractal dimension ($1 < D < 2$), $G$ the fractal roughness parameter and $\gamma$ is a scaling parameter ($\gamma > 1$). Eq. (4) represents the surface profile by a sum of cosine functions with geometrically increasing frequencies. In order for the phases of the different modes not to coincide at any given $x$ position, the value of $\gamma$ must be chosen to be a non-integer. Due to the self-affine property of fractals surfaces, $\gamma = 1.5$ can be assumed [21]. As $D$ becomes larger, the number of asperities increases (density increases) and their height decreases. As $G$ increases the peaks and the valleys are amplified, it therefore controls the asperities height. As the magnitudes of $D$ and $G$ increase, a rougher and more disordered surface topography can be generated.

Fractal representation of surface roughness has often been debated and authors do not all agree on its relevance. The main problem of using fractal representation for the topography of engineered surface is that not all of these surfaces are fractal. For refs. [22,23], the fractal character of artificial surfaces depends on the processing method. Fractals may, for example, not be applicable to very smooth surfaces [24]. The scale independence of the fractal parameters has moreover been questioned by refs. [22,24,25]. On the other hand, for ref. [26], many microfabricated surfaces can be represented by fractals. It has been shown that surfaces of processed steel, textured magnetic thin film [27], metallic ones produced by EDM, cutting or grinding techniques, and even worn surfaces are fractal [28]. Arguments in favor of the fractal characterization can be summarized by the necessity to characterize rough surfaces using intrinsic parameters independent of all scales of roughness.

## 5. Comparison with experiments

Works from Sacha et al. [29] and Hao et al. [14] are used to compare experimental results with results obtained using the simulation tool.

Sacha et al. measured electrostatic forces for a sphere-ended conical tip of radius 40 nm and half aperture angle 20° for different voltages. The characteristics of the tip were found using SEM images. Fig. 5 b gives a representation of the contact between the tip and a rough surface generated using a Weierstrass Mandelbrot function in the simulations. The experimental results are compared with simulations, first without and then with roughness parameters (fractal representation). Results are presented in Fig. 6. We first observed that even though the results are in good correlation, simulated forces are stronger in smooth configuration than what was experimentally obtained. Moreover, the difference between experimental results and simulation increases when the separation distance decreases. We attributed this observation

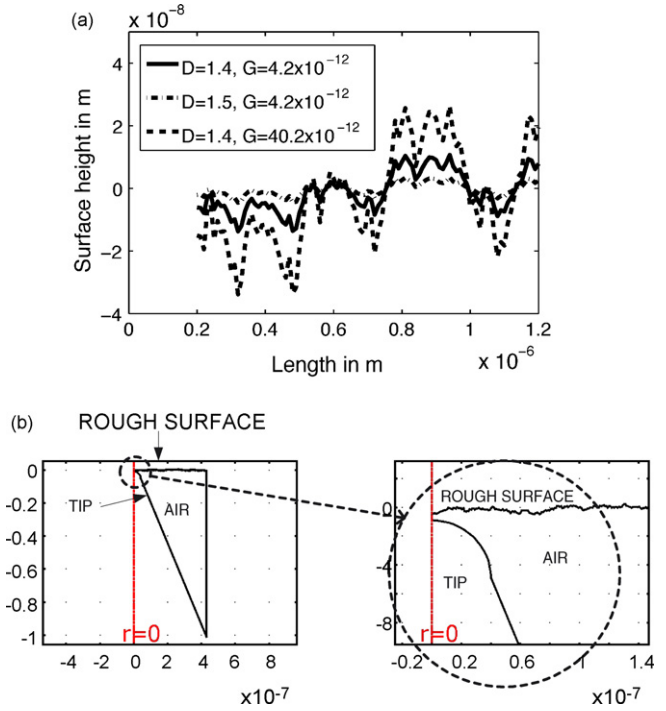


Fig. 5. (a) Illustration of the influence of the fractal parameters $D$ and $G$ on the profile and (b) contact between a conical tip and a rough surface during simulations.

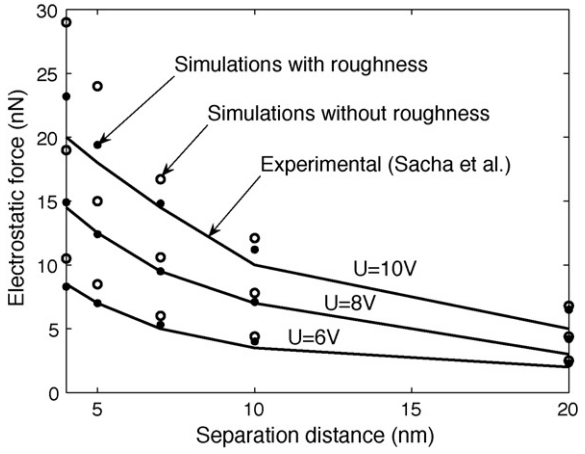


Fig. 6. Electrostatic normal force (nN) vs. separation distance (nm) for different voltages for a sphere-ended conical tip of radius 40 nm and half aperture angle $\theta = 20°$. Plot shows experimental results obtained by Sacha et al. [29], simulations results without roughness parameters and simulation results including roughness parameters $G = 5 \times 10^{-11}$ and $D = 1.8$ chosen in order to get maximum asperities height of the order of 1 nm.

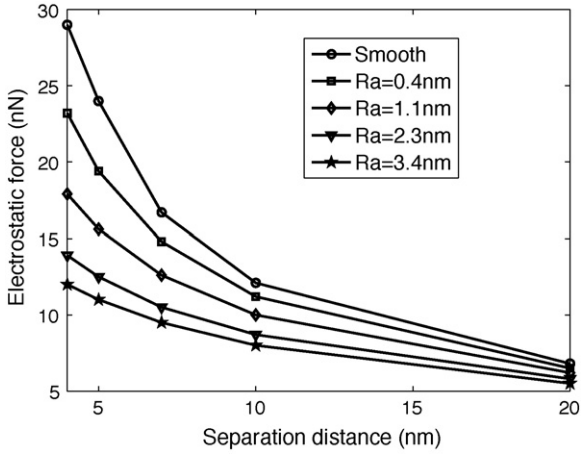


Fig. 8. Electrostatic normal force (nN) vs. separation distance (nm) for $U = 10$ V for a sphere-ended conical tip of radius 40 nm and half aperture angle $\theta = 20°$. Plot compares simulations results for the smooth configuration with simulations in rough configurations.

to the fact that even though the spot of contact has been chosen to be smooth, it can never be perfectly smooth. Even a very small roughness may influence the results at such small separation distances. We introduced roughness with the generation of a fractal surface using fractal parameters $D = 1.8$ and $G = 5 \times 10^{-11}$ for the planar contacting surface in order to have a maximum asperity peaks of 1.2 nm and an average roughness of 0.4 nm (which is often assumed to be negligible). These parameters have been chosen to correlate with Sacha et al. experiments where the contacting area has been chosen in order to have only monoatomic steps. The first observation is that even a roughness as small as this one is influencing the results from simulations, decreasing the electrostatic forces. This is specially true when the tip gets closer to the surface. The influence of surface roughness is also more important at higher applied voltages.

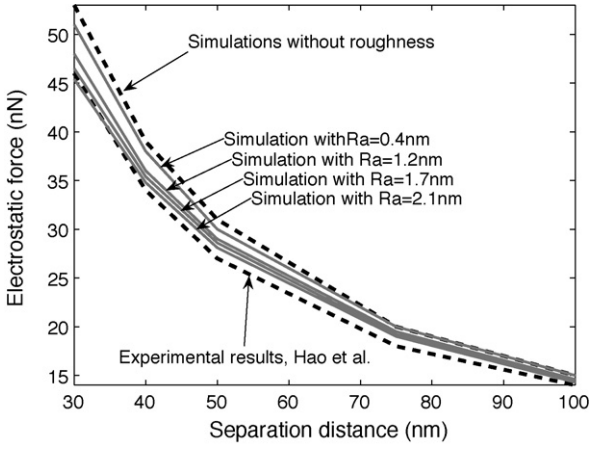


Fig. 7. Electrostatic normal force (nN) vs. separation distance (nm) for a sphere-ended conical tip of radius 270 nm and half aperture angle $\theta = 5°$. Plot shows experimental results obtained by Hao et al. [14], simulations results without roughness parameters and simulation results including different average roughness.

Hao et al. also measured electrostatic forces for a sphere-ended conical tip. The tip radius is 270 nm and the half aperture angle is 5°. Fig. 7 shows experimental results obtained compared with simulations for different roughness parameters. Conclusions are identical than what was observed for Sacha et al. The results from simulations including roughness are closer to the experimental measures. Roughness could thus be applied in micromanipulator design as a solution to decrease adhesion due to electrostatic forces. In Fig. 8 are shown more results of simulations for a conical tip ($R = 40$ nm, $\theta = 20°$). The force is decreased by half at close separation distances ($d = 4$ nm) with only an average roughness of 2.3 nm.

## 6. Application case

Fig. 9 illustrates how simulations can be used to improve a microgripper design by studying the influence of parameters such as geometry of the end-effectors, geometry of the handled object, materials, fabrication process and surface treatments (polishing, roughening, coating). Taking deformations into account will be in the next step of the development. The simulation tool is used for the application case of the two-figured gripper [6] (Fig. 1). The dimensions of the end-effectors are 1 mm × 0.2 mm × 0.3 mm. The microgripper is made of nickel. The simulations are performed for the manipulation of a silver cylinder of dimensions $R = 25$ μm and $L = 0.2$ mm. When the two dissimilar metals are brought into contact, they exchange electrons in such a way as to equilibrate their Fermi levels in order to bring the system in thermodynamic equilibrium. The potential difference resulting once the equilibrium has been reached at the interface of the contacting solids is the contact potential difference and is estimated to be 0.2 V between nickel and silver. Contact occurs at the interatomic separation distance between surfaces which is 0.5 nm [30]. From results shown in Fig. 10, adhesion

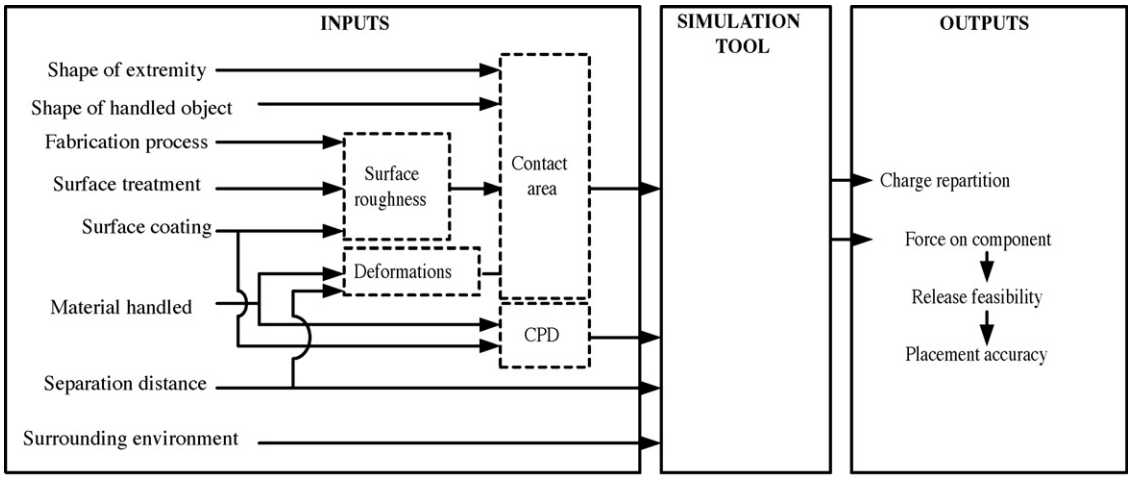


Fig. 9. Strategies for improving microgripper design.

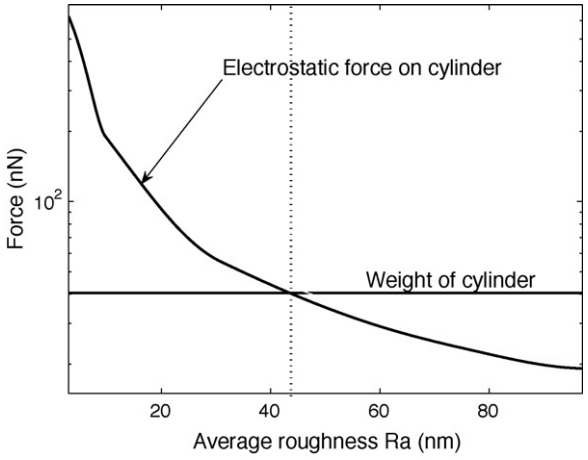


Fig. 10. Electrostatic force between the end-effectors of a flat micromanipulator [6] and a silver cylinder ($R = 25$ μm and $L = 0.2$ mm): electrostatic force as a function of the average roughness on the manipulator ($U = 0.2$ V, $d = 0.5$ nm).

due to electrostatic forces is overcame by gravity when an average surface roughness of at least 43 nm is applied.

## 7. Conclusion

Analytical models for electrostatic forces evaluation were reviewed. These models are very restricted in shape and do not take surface roughness into account. They are thus not easily applicable to micromanipulations and micromanipulator design. Simulations were performed using Comsol to solve the Laplace equation with the finite elements method and Matlab to generate rough surfaces using the Weierstrass Mandelbrot function. The aim is to predict electrostatic forces between a gripper end-effectors and a grasped object in order to improve the gripper design and avoid adhesive disturbing effects due to electrostatic forces. Simulations showed good correspondence with analytical models in smooth configurations and gave encouraging results for the validity of the simulation tool. It allows to implement any geometry and a wide range of separation distances without decreasing the accuracy of the results. The first simulations including roughness parameters compared with experimental results showed good correlation and demonstrate the need not to neglect surface topography in electrostatic forces calculations because it is an important parameter in modeling adhesion [31]. Roughness causes contact only to happen on the peaks of asperities and thus reduces the area of contact. Surface roughness has the effect of reducing the area of contact between the surfaces and consequently reduces the electrostatic interaction. Deformations will also change the contacting area and will have an influence on electrostatic forces. This is part of our prospective work. The accuracy of using fractal representation for the surface topography of micromachined materials has also to be confirmed.

## Acknowledgement

This work was sponsored by the Communauté Française de Belgique within the framework of an Action de Recherche Concertée (convention 04/09-310).

## References

[1] J. Agnus, Contribution à la micromanipulation: Etude, réalisation, caractérisation et commande d'une micropince piézoélectrique, Ph.D. thesis, Laboratoire d'Automatique de Besançon (UMR CNRS 6596), 2003.
[2] Y. Rollot, S. Régnier, J.C. Guinot, Simulation of micromanipulations: adhesion forces and specific dynamic models, Int. J. Adhes. Adhes. 19 (1) (1999) 35–48.
[3] D.S. Haliyo, Les forces d'adhésion et les effets dynamiques pour la micromanipulation, Ph.D. thesis, Université Pierre et Marie Curie, 2002.
[4] P. Lambert, S. Régnier, Surface and contact forces models within the framework of microassembly, J. Micromechatronics 3 (2) (2006) 123–157.
[5] M. Gauthier, S. Régnier, P. Rougeot, N. Chaillet, Analysis of forces for micromanipulations in dry an dliquid media, J. Micromechatronics 3 (2006) 389–413.
[6] J. Agnus, P.G.D. Lit, C. Clévy, N. Chaillet, Description and performances of a four-degrees-of-freedom piezoelectric gripper, in: Proceedings of the Fifth IEEE International Conference on Assembly and Task Planning (ISATP2003), Besançon, France, (2003), pp. 66–72.

[7] R.S. Fearing, Survey of sticking effects for micro parts handling, in: Proc. of IEEE/RSJ Conf. on Intelligent Robots and Systems, 1995, 212–217.
[8] R.A. Bowling, A theoretical review of particle adhesion, in: Proc. of symposium on particles on surfaces 1: detection, adhesion and removal, San Francisco, (1986), pp. 129–142.
[9] S. Belaidi, P. Girard, G. Leveque, Electrostatic forces acting on the tip in atomic force microscopy: modelization and comparison with analytic expressions, J. Appl. Phys. 81 (3) (1997) 1023–1029.
[10] B. Cappella, G. Dietler, Force–distance curves by atomic force microscopy, Surf. Sci. Rep. 34 (1999) 1–104.
[11] S. Hudlet, M.S. Jean, J. Berger, Evaluation of the capacitive force between an atomic force microscopy tip and a metallic surface, Eur. Phys. J. B 2 (1998) 5–10.
[12] H.-J. Butt, B. Cappella, M. Kappl, Force measurements with atomic force microscope: technique, interpretation and applications, Surf. Sci. Rep. 59 (2005) 1–152.
[13] E. Durand, Electrostatique: Tome II Problèmes généraux, Conducteurs, Masson, 1966.
[14] H.W. Hao, A.M. Baro, J.J. Saenz, Electrostatic and contact forces in force microscopy, J. Vacuum Sci. Technol. B 9 (2) (1991) 1323–1328.
[15] S. Patil, A. Kulkarni, C. Dharmadhikari, Study of the electrostatic force between a conducting tip in proximity with a metallic surface: theory and experiment, J. Appl. Phys. 88 (11) (2000) 6940–6942.
[16] S. Patil, C. Dharmadhikari, Investigation of the electrostatic forces in scanning probe microscopy at low bias voltage, Surf. Interf. Anal. 33 (2002) 155–158.
[17] E. Bonaccurso, F. Schönfeld, H. Butt, Electrostatic forces acting on tip and cantilever in atomic force microscopy, Phys. Rev. B 74 (2006) 1–8.
[18] J. Colchero, A. Gile, A. Baró, Resolution enhancement and improved data interpretation in electrostatic force microscopy, Phys. Rev. B 64 (2001) 245403.
[19] B. Law, F. Rieutord, Electrostatic forces in atomic force microscopy, Phys. Rev. B 66 (035402-1).
[20] M.V. Berry, Z.V. Lewis, On the Weierstrass-Mandelbrot fractal function, Proc. R. Soc. Lond. Ser. A 370 (1980) 459–484.
[21] K. Komvopoulos, A fractal analysis of stiction in microelectromechanical systems, J. Tribol. 119 (3) (1997) 391–400.
[22] L. He, J. Zhu, The fractal character of processed metal surfaces, Wear 208 (1997) 17–24.
[23] D.J. Whitehouse, Fractal or fiction, Wear 249 (5–6) (2001) 345–353.
[24] S. Eichenlaub, A. Gelb, S. Beaudouin, Roughness models for particle adhesion, J. Colloid Interface Sci. 280 (2004) 289–298.
[25] S. Ganti, B. Bhushan, Generalized fractal analysis and its applications to engineering surfaces, Wear 180 (1994) 17–34.
[26] K. Komvopoulos, Surface engineering and microtribology for microelectromechanical systems, Wear 200 (1) (1996) 305–327.
[27] A. Majumdar, C. Tien, Fractal characterization and simulation of rough surfaces, Wear 136 (1990) 313–327.
[28] H. Zhu, S. Ge, X. Huang, D. Zhang, J. Liu, Experimental study on the characterization of worn surface topography with characteristic roughness parameter, Wear 255 (2003) 309–314.
[29] G. Sacha, A. Verdaguer, J. Martinez, J. Sáenz, D. Ogletree, M. Salmeron, Effective radius in electrostatic force microscopy, Appl. Phys. Lett. 86 (2005) 123101.
[30] J.N. Israelachvili, The nature of van der Waals forces, Contemp. Phys. 15 (2) (1974) 159–177.
[31] W.M. van Spengen, R. Puers, I.D. Wolf, A physical model to predict stiction in mems, J. Micromech. Microeng. 12 (5) (2002) 702–713.

Please cite this article in press as: M.S. Lhernould et al., Electrostatic forces in micromanipulations: Review of analytical models and simulations including roughness, Appl. Surf. Sci. (2007), doi:10.1016/j.apsusc.2007.01.098